# Disrupted PI3K subunit p110α signaling protects against pulmonary hypertension and reverses established disease in rodents

Eva M. Berghausen[1,2,3], Wiebke Janssen[4,5], Marius Vantler[1,2,3], Leoni Feik[1,2,3], Max Krause[1,2,3], Arnica Behringer[1,2], Christine Joseph[1,2], Mario Zierden[1,2,3], Henrik ten Freyhaus[1,2,3], Anna Klinke[1,2,3], Stephan Baldus[1,2,3], Miguel A. Alcazar[2,6,7], Rajkumar Savai[4], Soni Savai Pullamsetti[4], Dickson W.L. Wong[8], Peter Boor[8], Jean J. Zhao[9], Ralph T. Schermuly[4,5], Stephan Rosenkranz[1,2,3,*]

[1]Dept. of Cardiology, Heart Center at the University of Cologne, Germany
[2]Center for Molecular Medicine Cologne (CMMC); University of Cologne, Germany
[3]Cologne Cardiovascular Research Center (CCRC), University of Cologne, Germany
[4]Max-Planck Institute for Heart and Lung Research, Bad Nauheim, Germany
[5]Universities of Giessen and Marburg Lung Center (UGMLC), Giessen, Germany, and German Centre for Lung Research (DZL)
[6]Institute for Lung Health, Member of the German Centre for Lung Research (DZL), University of Giessen and Marburg Lung Centre (UGMLC), Giessen, Germany
[7]Department of Children and Adolescent Medicine, University of Cologne, Germany
[8]Institute of Pathology, RWTH Aachen University Hospital, Aachen, Germany
[9]Dana Farber Cancer Center, Havard Medical School, Boston, MA
* corresponding author

## SUPPLEMENTARY MATERIAL

**Content:**

## SUPPLEMENTARY METHODS

### Human samples – Patient information

Human lung samples and patient characteristics. Human explanted lung tissues from subjects with idiopathic PAH (IPAH) (n=16) or control donors (n=14) were obtained during lung transplantation. Subjects with idiopathic PAH had a mean age (years ± SD) of 30.3 ± 11.9; Ten were females, six were males. The mean (±SD) pulmonary artery pressure was 65.1 ± 20.8 mmHg. Control donors had a mean age (years ± SD) of 43.8 ± 16.6; Six were females, eight were males. Samples of donor lung tissue were taken from the lung that was not transplanted. The study protocol for tissue donation was approved by the ethics committee (Ethik-Kommission am Fachbereich Humanmedizin der Justus-Liebig-Universität Gießen) of the University Hospital Gießen (Gießen, Germany) in accordance with national law and with Good Clinical Practice/International Conference on Harmonisation guidelines. Written informed consent was obtained from each individual patient or the patient's next of kin (AZ 31/93). All lungs were reviewed for pathology, and the IPAH lungs were classified as grade III or IV according to Heath & Yacoub (*J Clin Pathol 1991;*44:1003-1006).

### Immunofluorescence staining of phosphorylated PDGFRβ

The FFPE lung tissues were deparaffinized and rehydrated with a concentration gradient of ethanol. Heat-Induced Epitope Retrieval step was performed with Antigen Unmasking Solution (Vector Laboratories, Burlingame, CA, USA), followed by incubation with primary antibody against p-PDGFRβ antibody (H-8) (1:100, Santa Cruz Biotechnology, Dallas, TX, USA) and Alexa Fluor® 647 AffiniPure Rabbit Anti-Mouse IgG (1:200, Jackson ImmunoResearch Europe Ltd, Cambridge, UK) was used as the secondary antibody. Nuclei were labeled with DAPI (Sigma-Aldrich, St. Louis, MO, US) and the slides were mounted with ProLong™ Gold antifade reagent (Invitrogen, Waltham, MA). Mouse IgG (Vector Laboratories, Burlingame, CA) was used as a negative control for the primary antibody.

### Fluorescence *In Situ* Hybridization (FISH) of PDGFRβ

The FFPE lung tissues were deparaffinized followed by dehydration with 100% ethanol. FISH was performed with the RNAscope® Multiplex Fluorescent Reagent Kit v2 assay (Advanced Cell Diagnostics, Inc., Hayward, California). Briefly, we incubated the tissue sections with $H_2O_2$ before the heat-induced target retrieval step and protease incubation. *PDGFRB* mRNA and the negative control slide was hybridized with the RNAscope® Probe- Hs-PDGFRB (#548991) and the negative probe, respectively. After several signal amplification steps, Opal™ 650 fluorophores (PerkinElmer Life and Analytical Sciences, Boston, MA) was applied. For co-staining with phosphorylated PDGFRβ, similar experimental steps were performed as mentioned above, except Alexa Fluor 555 conjugated anti-mouse secondary antibody was used. The stained tissues were analyzed with Zeiss Axio Imager 2 and image analysis software (ZEN 3.0 blue edition).

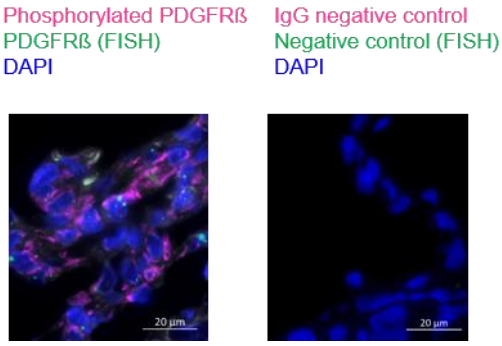


**Supplementary Figure 1. Control stainings for phosphorylated PDGFRß.**
Scale bar = 20µm.

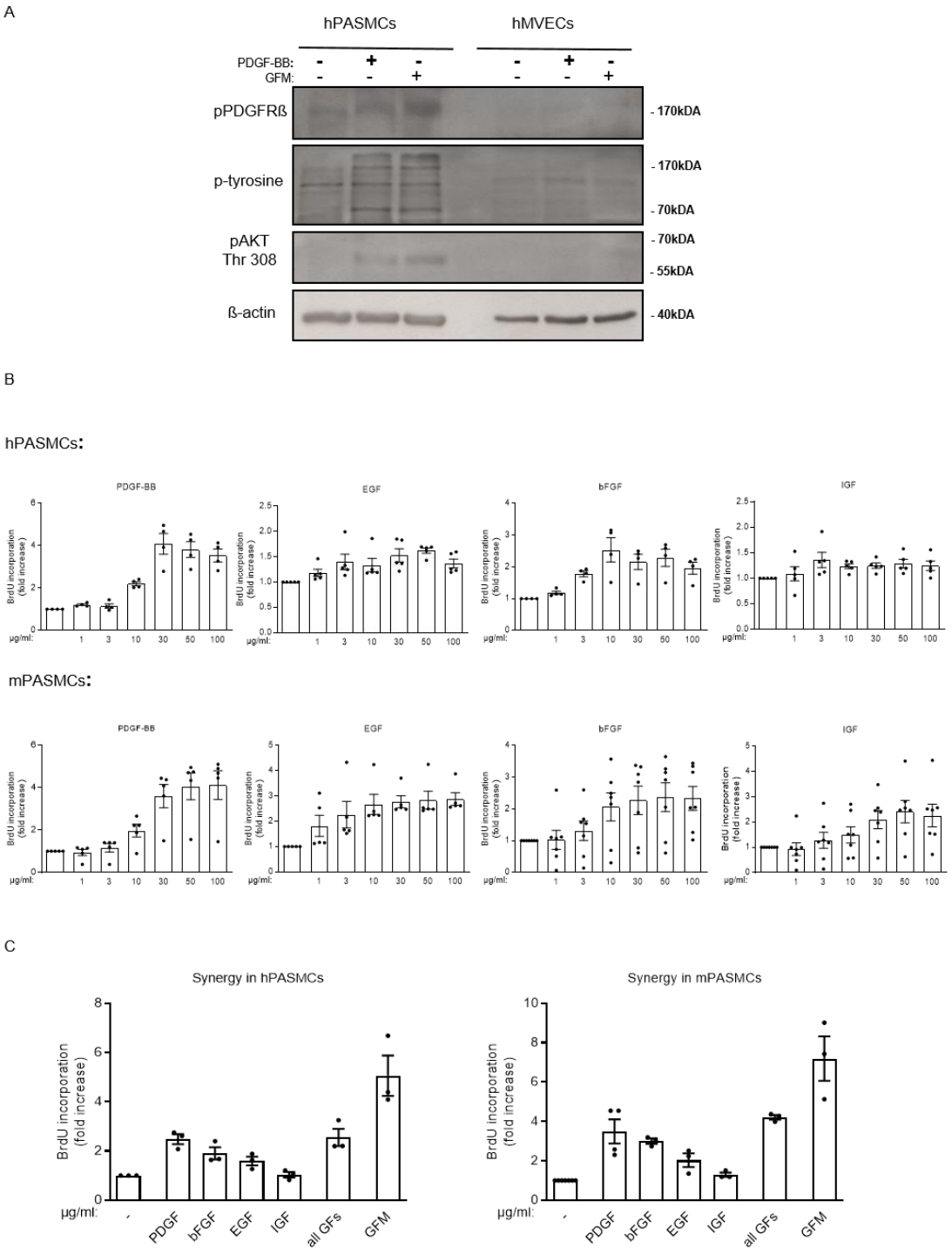


**Supplementary Figure 2. Cell-type specific effects of various growth factors. (a)** Western blot demonstrating the phosphorylation of the PDGFß receptor, tyrosine residues (Y) and AKT in human PASMCs and human microvascular endothelial cells (hMVECs) stimulated by either PDGF-BB or smooth muscle basal medium (SmBm: FGF [2ng/ml], EGF [0,5 ng/ml], Insulin [0,5µg/ml], FCS 5%) with PDGF-BB [30ng/ml], referred to as growth factor mixture (GFM). **(b)** Dose-relation of growth factor induced PASMC proliferation. Proliferation in response to the indicated concentrations of PDGF-BB, EGF, bFGF and IGF in human (left panel) and mouse (right panel) PASMCs (n=4-7 each). **(c)** Synergistic effects of growth factors on PASMC proliferation. Proliferation in response to PDGF-BB, EGF, bFGF and IGF alone [each 30ng/ml], in combination, and GFM in human (left panel) and mouse (right panel) PASMCs (n=3-4 each).

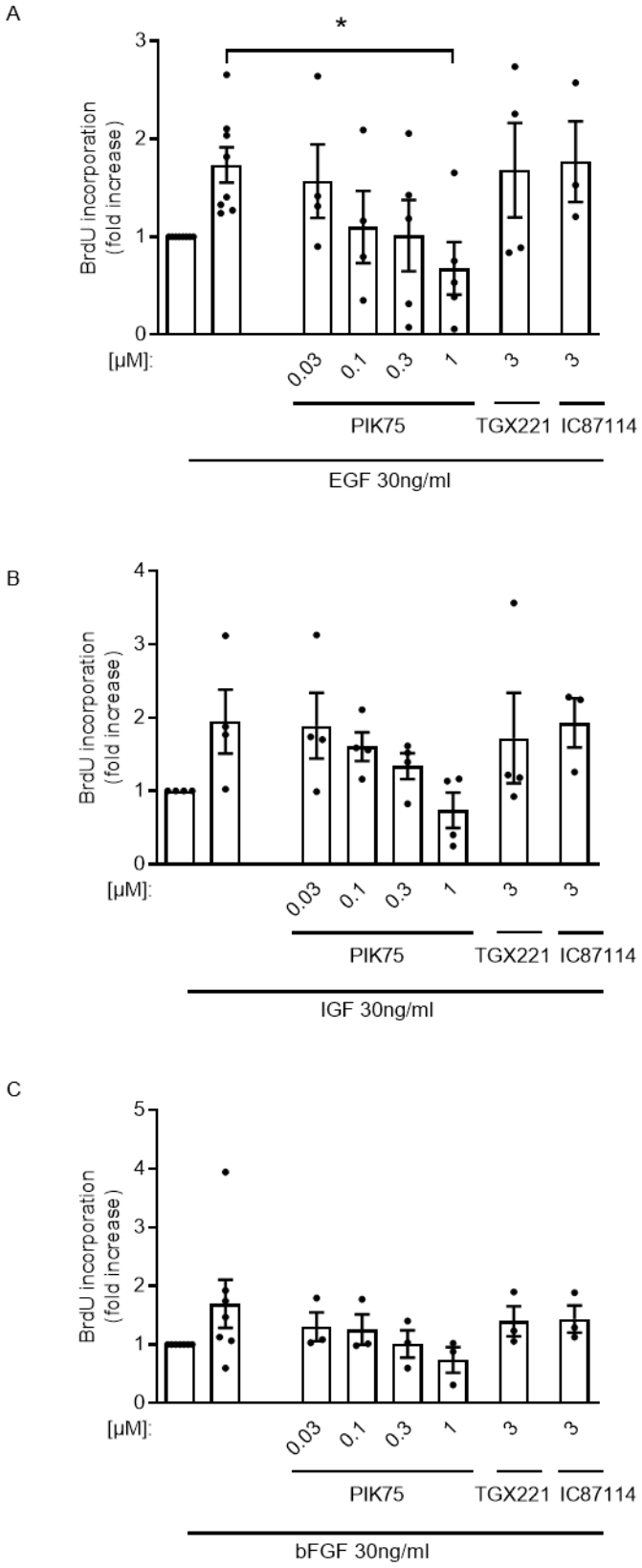


**Supplementary Figure 3. Effects of isoform-specific PI3K inhibitors on proliferation induced by EGF, IGF and bFGF.** Starved human PASMCs were pre-incubated with the indicated inhibitors and stimulated with EGF [30ng/ml] (n=3-5) **(a)**, IGF-I [30ng/ml] (n=3-5) **(b),** or basic FGF [30ng/ml] (n=3-7) **(c)**. Proliferation was determined by BrdU incorporation. Data were normalized to starved controls and represent means ± SEM. **p*<0.05 versus growth factor alone as assessed by one-way ANOVA with Dunnett´s test.

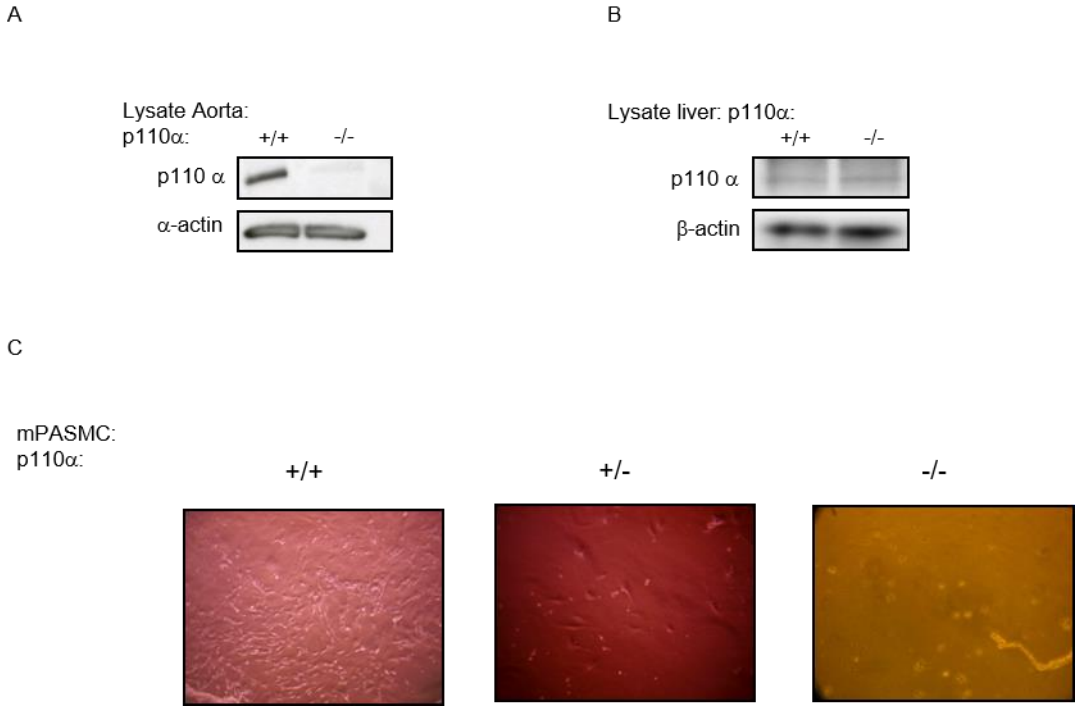


**Supplementary Figure 4. Proof of principal: SM-specific p110α deficiency in aorta and liver. (a)** Western blots showing the expression of p110α in the aorta of smooth muscle-specific p110α-deficient mice in comparison to wild type control mice. α-actin is shown as a loading control. **(b)** Western blots showing similar expression of p110α in liver homogenates from sm-p110$\alpha^{-/-}$ mice compared to wild type controls. ß-actin is shown as loading control. **(c)** Representative images of PASMCs 7 days after isolation, demonstrating reduced proliferation of p110α-deficient cells under tissue culture conditions. Cells were seeded into a 24 well-plate in DMEM containing 20% FCS and penicillin / streptomycin.

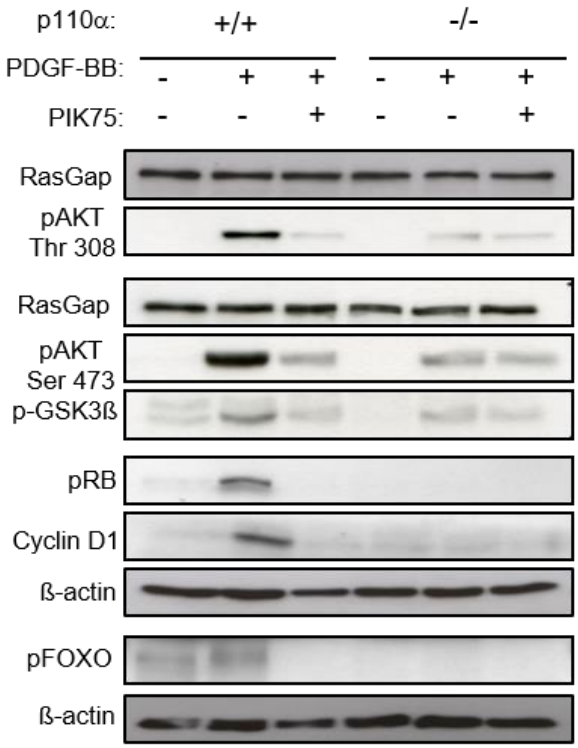


**Supplementary Figure 5. Effects of PIK75 on PDGF-BB-dependent downstream signaling in p110α deficient versus wild type mPASMCs.** Starved mPASMCs were preincubated with DMSO or PIK75 and stimulated with PDGF-BB [30ng/ml] for 5 minutes (pAKT, pGSK3β) or 16 hours (pRb, cyclin D1, pFOXO), respectively. Blots were probed with the indicated antibodies. RasGAP and ß-actin are shown as loading control.

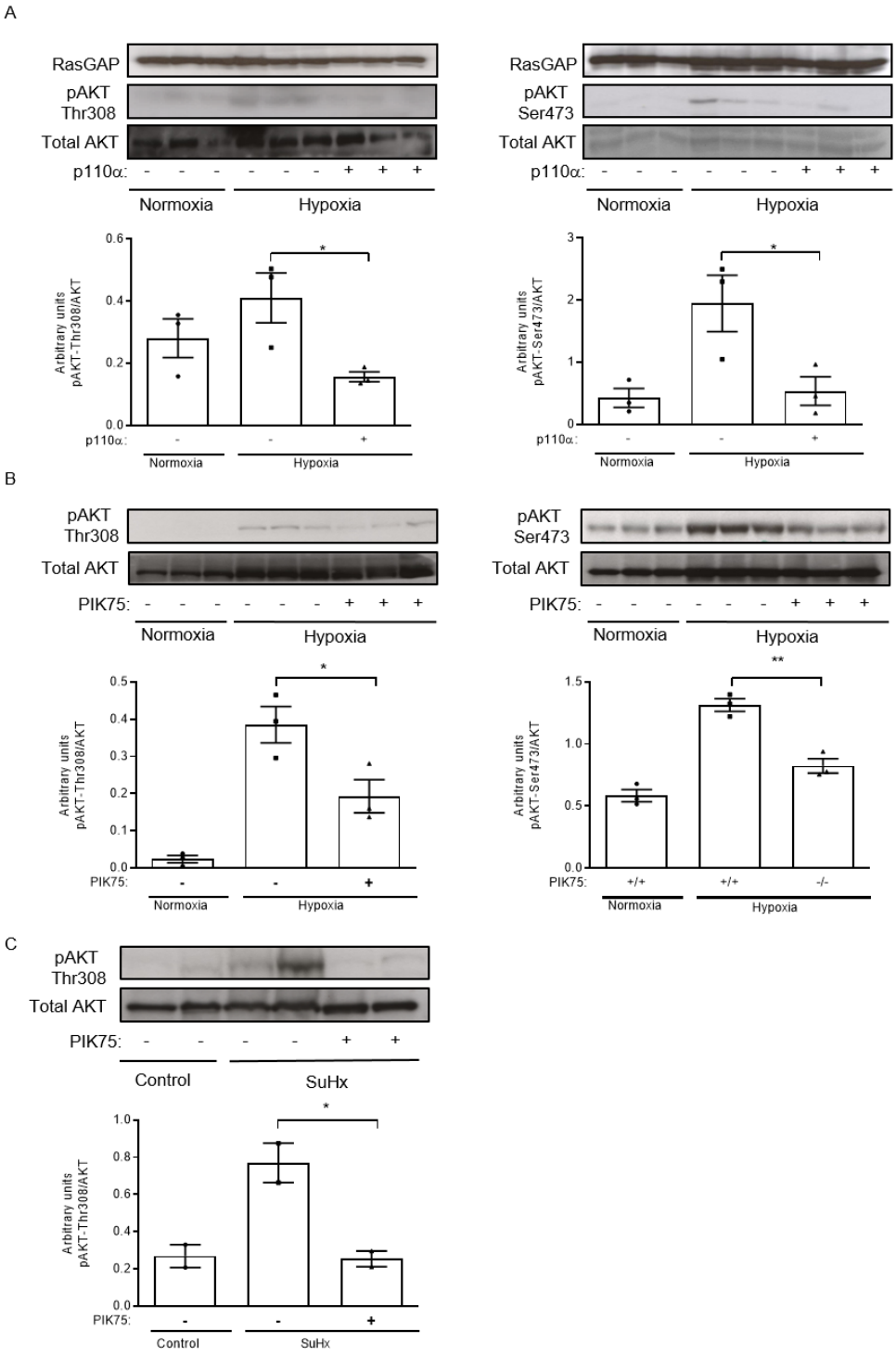


**Supplementary Figure 6. Blunting of p110α signaling prevents phosphorylation of AKT in lung tissue in experimental PH. (a)** SM-specific lack of p110α prevents phosphorylation of AKT in hypoxia challenged mice. Phosphorylation of AKT (Thr308) (left) and of AKT (Ser473) (right) in normoxic p110α$^{+/+}$ and hypoxic p110α$^{+/+}$ and p110α$^{-/-}$ mice. **(b)** Inhibition of p110α using PIK75 prevents phosphorylation of AKT in lung tissue of hypoxia challenged mice. Phosphorylation of AKT (Thr308) (left) and of AKT (Ser473) (right) in normoxic and hypoxic vehicle and PIK75 treated mice. **(c)** Inhibition of p110α using PIK75 reduces phosphorylation of AKT in lung tissue of SuHx rats. Phosphorylation of AKT (Thr308) in vehicle and PIK75 treated control and SuHx challenged rats. RasGAP and total AKT are shown as a loading control. Quantification was performed by densitometric analysis. Data represent means ± SEM. **p*<0.05;***p*<0.01 as assessed by one-way ANOVA with Dunnett´s test.

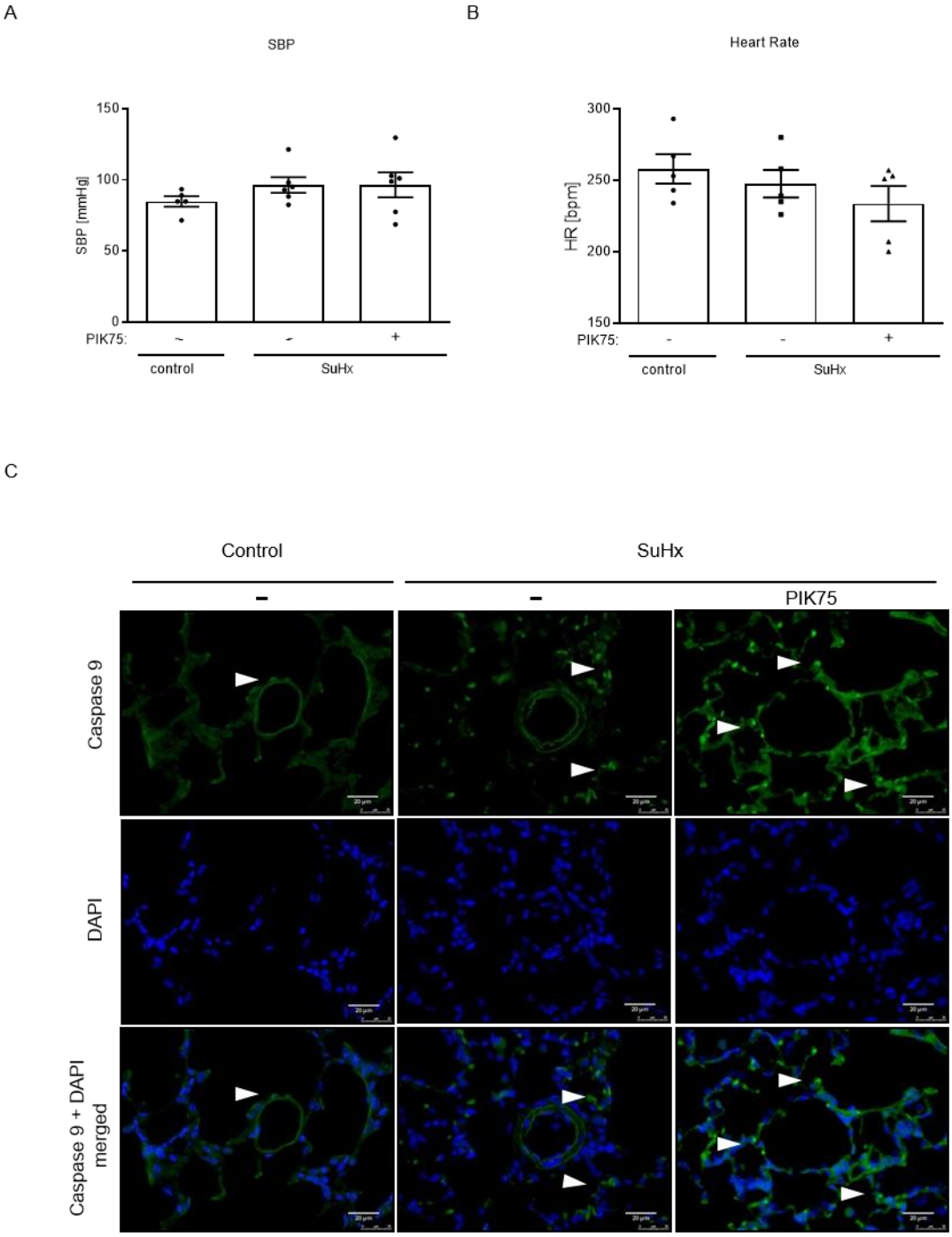


**Supplementary Figure 7. Effects of p110α inhibition on circulatory measures, and vascular apoptosis in the Su/Hx model. (a)** Systolic blood pressure (SBP) [mmHg] (n=5-6); **(b)** heart rate [bpm] in untreated or PIK75-treated Sugen/hypoxia exposed rats in comparison to controls (n=5 each). **(c)** Representative immunofluorescence photomicrographs of Caspase (green) and DAPI (blue) in small pulmonary vessels from rats. Scale bar = 20 µm. Arrowheads indicate TUNEL positive cells. Data represent means ± SEM.

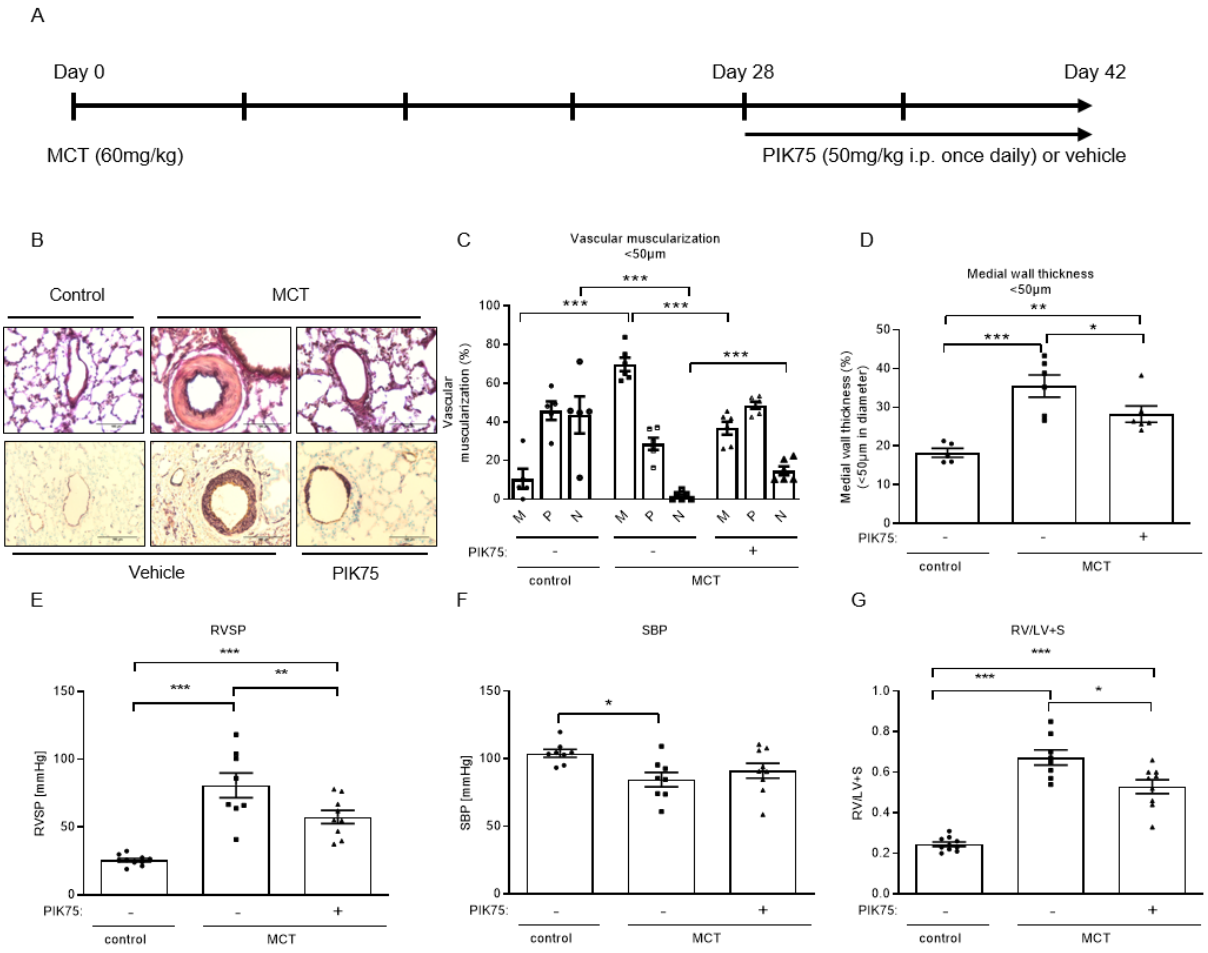


**Supplementary Figure 8. Therapeutic inhibition of p110α with PIK75 reverses monocrotalin (MCT)-induced pulmonary hypertension. (a)** Schematic diagram illustrating the treatment protocol in the MCT model. **(b)** Double-immunostaining for von Willebrand factor (vWF, brown) and α-smooth muscle actin (purple) demonstrating the muscularization (upper panel) of peripheral pulmonary arteries or Van-Gieson staining demonstrating medial wall thickness (lower panel) in control animals versus untreated or PIK75-treated rats with MCT-induced pulmonary hypertension. Shown are representative images of lung sections. Scale bar = 100µm. **(c)** Impact of p110α inhibition with PIK75 on vascular muscularization of small pulmonary arteries (<50 µm). Shown is the percentage of fully (M), partially (P) and non muscularized (N) vessels (at least 80 were analyzed per animal) (n=5-6)**. (d)** Medial wall thickness of <50µm sized pulmonary arteries (n=5-6)**, (e)** right ventricular systolic pressure (RVSP) [mmHg (n=8-10), **(f)** systolic blood pressure (SBP) [mmHg], (n=8-9), and **(g)** right ventricular (RV) hypertrophy in MCT-treated rats compared to controls,(n=8-10). Data represent means ± SEM. **p*<0.05; ***p*<0.01; ****p*<0.001 as assessed by ANOVA followed by Newman-Keuls post-hoc test.

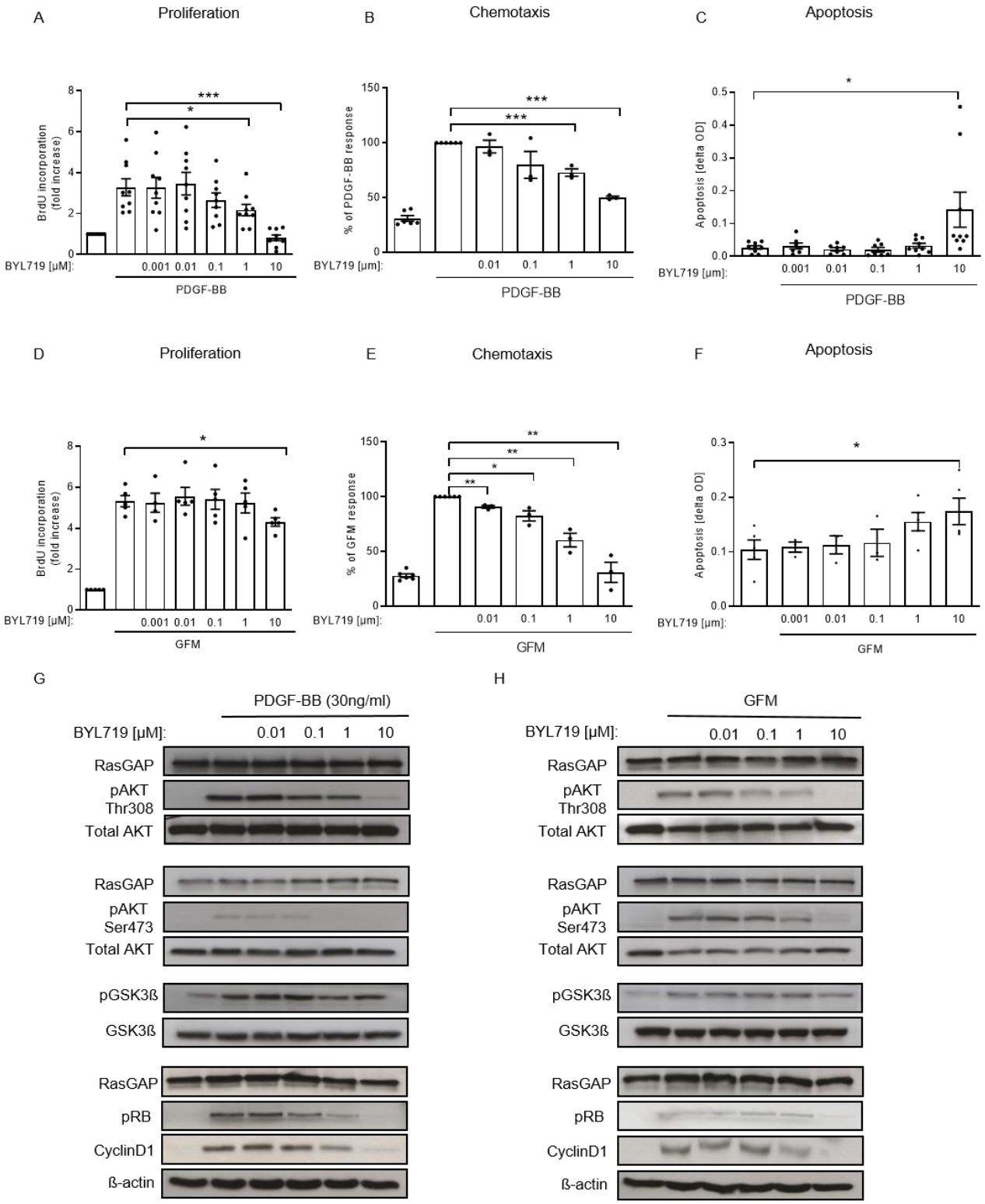


**Supplementary Figure 9. BYL719 attenuates growth factor-induced responses in human PASMCs.** PDGF-BB [30 ng/ml]-dependent **(a)** proliferation (n=9), **(b)** chemotaxis (n=3-6), and **(c)** apoptosis (n=6-9) of hPASMCs in the presence of BYL719 in the indicated concentrations. **(d)** Proliferation (n=5), **(e)** chemotaxis (n=3-6) and **(f)** apoptosis (n=3-5) of growth factor mixture (GFM)-stimulated hPASMCs in the absence or presence BYL719. Data represent means ± SEM. **p*<0.05; ***p*<0.01; ****p*<0.001 as assessed by one-way ANOVA with Dunnett´s test. Impact of BYL719 in the indicated concentrations on **(g)** PDGF-BB [30ng/ml] or **(h)** GFM-induced downstream signaling events in hPASMCs. Shown is the phosphorylation of AKT (Thr 308 and Ser 473), GSK3ß and RB and expression of CyclinD1. RasGAP, total AKT, total GSK3ß and ß-actin are shown as loading controls.

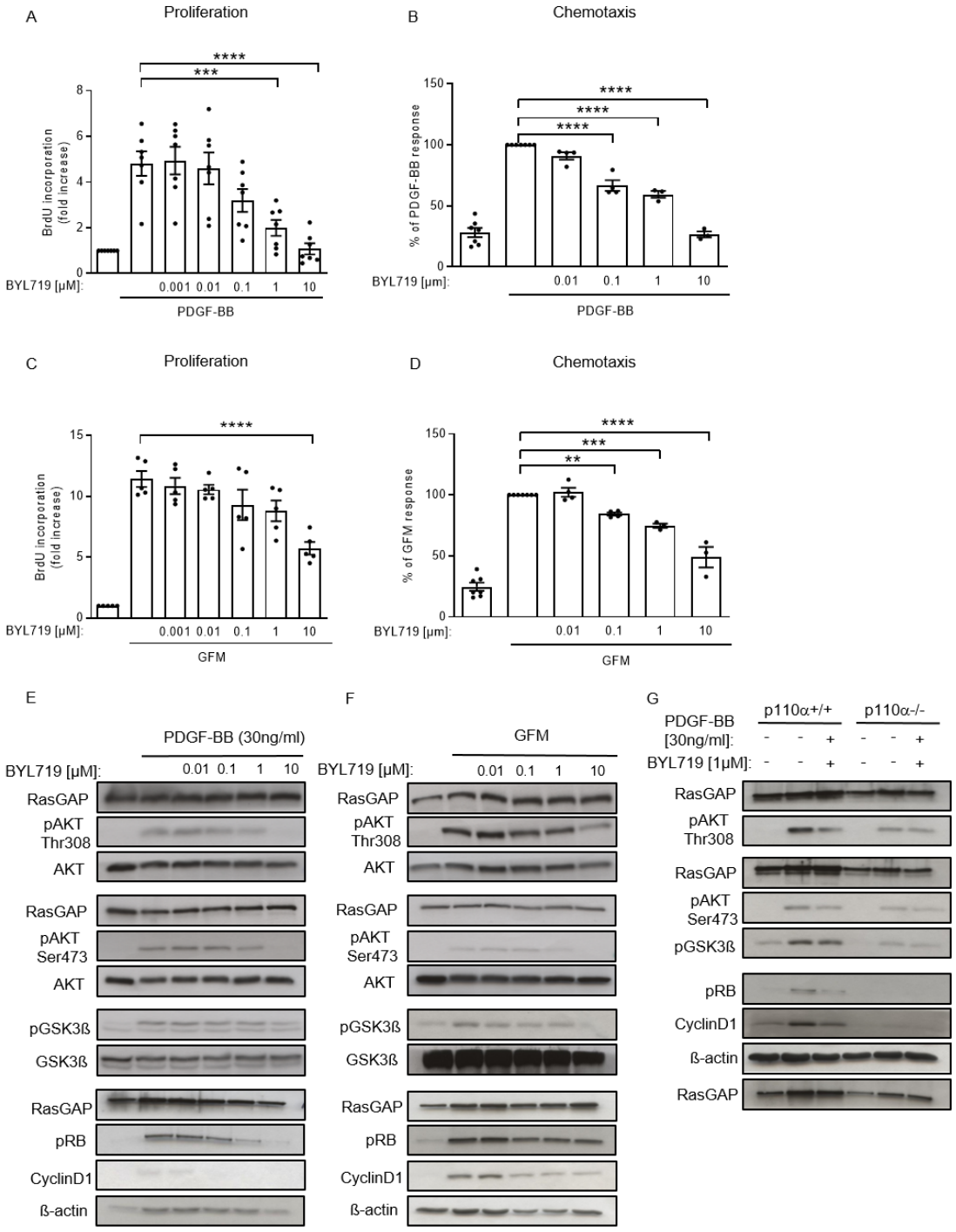


**Supplementary Figure 10. BYL719 attenuates growth factor-induced responses in murine PASMCs.** PDGF-BB [30 ng/ml]-dependent **(a)** proliferation (n=7) and **(b)** chemotaxis (n=4-7) of mPASMCs in the presence of BYL719 in the indicated concentrations. **(c)** Proliferation (n=5) and **(d)** chemotaxis (n=3-7) of growth factor mixture (GFM)-stimulated hPASMCs in the absence or presence of BYL719. Data represent means ± SEM. **p*<0.05; ***p*<0.01; ****p*<0.001, *****p*<0.0001 as assessed by one-way ANOVA with Dunnett´s test. Impact of BYL719 in the indicated concentrations on **(e)** PDGF-BB [30ng/ml] or **(f)** GFM-induced downstream signaling events in mPASMCs. Shown is the phosphorylation of AKT (Thr 308 and Ser 473), GSK3ß and RB and expression of CyclinD1. RasGAP, total AKT, total GSK3ß and ß-actin are shown as loading controls. **(g)** Effects of BYL719 on PDGF-BB-dependent downstream signaling in p110α deficient versus wild type mPASMCs. Starved mPASMCs were preincubated with DMSO or BYL719 and stimulated with PDGF-BB [30ng/ml] for 5 minutes (pAKT, pGSK3β) or 16 hours (pRb, cyclin D1), respectively. Blots were probed with the indicated antibodies. RasGAP, ß-actin,total AKT and total GSK3ß are shown as loading controls.

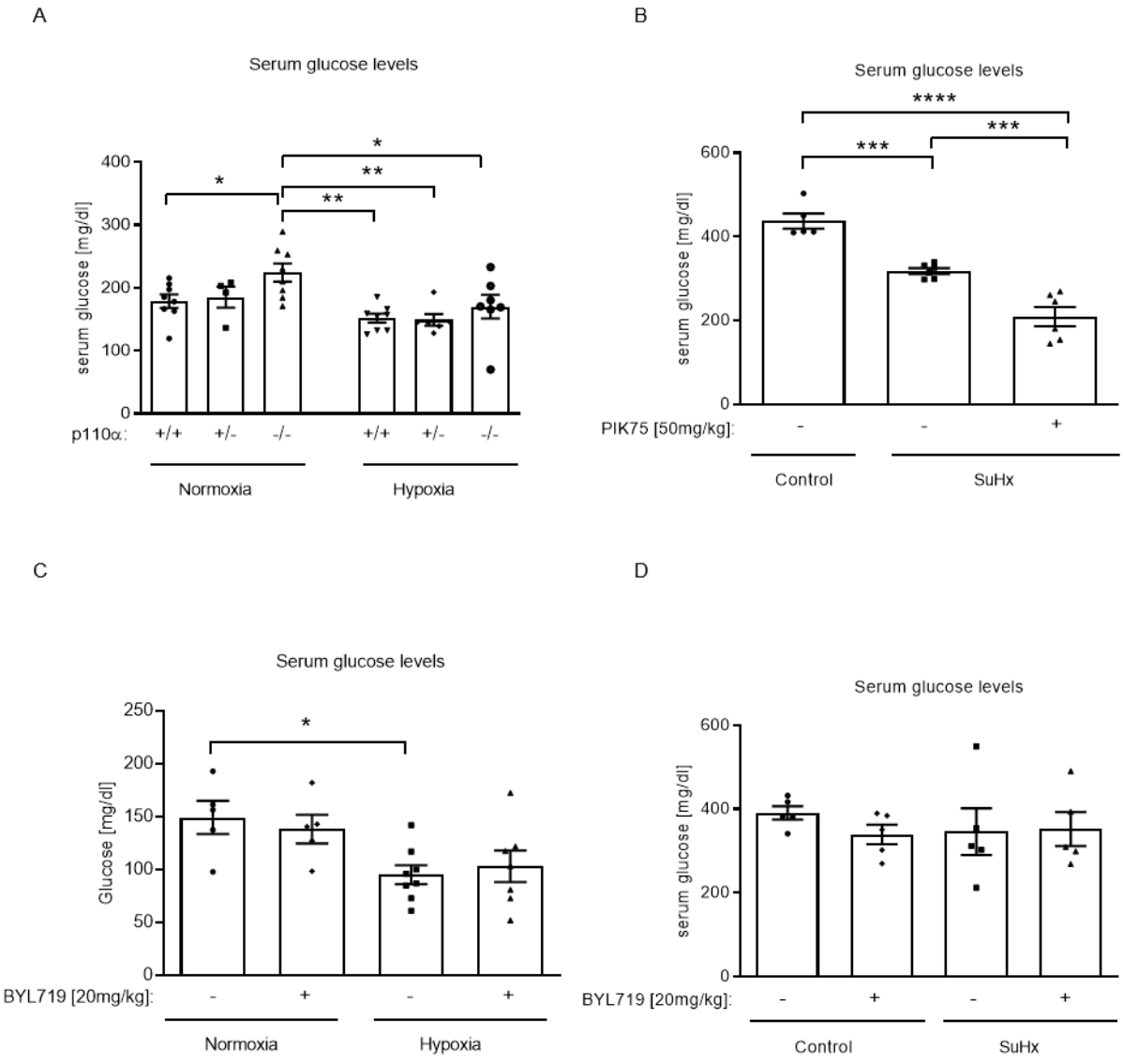


**Supplementary Figure 11. Serum glucose levels of p110α$^{-/-}$ mice and PIK75 or BYL719 treated mice or rats.** Serum samples taken after hemodynamic characterisation of **(a)** normoxic and hypoxic p110α$^{+/+}$, $^{+/-}$ and $^{+/+}$ mice (n=6-8), **(b)** vehicle or PIK75 treated rats in the SuHx model (n=5-6); **(c)** normoxic and hypoxic vehicle or BYL719 treated mice (n=5-7), and **(d)** rats (n=5 each). Data represent means ± SEM. *$p$<0.05; **$p$<0.01; ***$p$<0.001, ****$p$<0.0001 as assessed by ANOVA followed by Newman-Keuls post-hoc test.